5-3-2012

Locking Down The N-Terminus of PRMT1 In Order To Assess The Role Of Motion In Activity

Taylor James Rasmussen
Utah State University

LOCKING DOWN THE N-TERMINUS OF PRMT1 IN ORDER TO ASSESS THE ROLE OF MOTION IN ACTIVITY

by

Taylor James Rasmussen

Thesis submitted in partial fulfillment
of the requirements for the degree

of

DEPARTMENTAL HONORS

in

Biochemistry
in the Department of Chemistry & Biochemistry

Approved:

Thesis/Project Advisor	**Departmental Honors Advisor**
Dr. Joan M. Hevel	Dr. Alvan C. Hengge

Director of Honors Program
Dr. Christie Fox

UTAH STATE UNIVERSITY
Logan, UT

Spring 2012

Abstract

Protein arginine methyltransferases (PRMTs) are involved in many major biological pathways in the human body. Processes that demonstrate arginine methylation by PRMTs include, but are not limited to, histone modification, DNA transcription, and post-translational protein modifications. Although recent research has allowed the identification of several PRMT isoforms and exposed their involvement in these processes, relatively little is known about the details of how these enzymes perform their biochemical duties. It is currently hypothesized that the N-terminus of PRMT variant 1 is involved in recognizing substrates and aiding in catalysis by virtue of a change in its conformation. To understand how the N-terminal tail (Nt) of human PRMT1 may influence substrate recognition, we made a mutant of rat PRMT1 where the N-terminus could hypothetically be switched from a "locked down" conformation into a "free" conformation using a simple small molecule. After sequence confirmation of the mutations, different expression parameters were tested to determine optimal expression. The mutant protein was then purified from the soluble portion of the expression cell growth using Ni affinity techniques. Activity was assessed in the presence and absence of the small molecule diothiothreitol (DTT). The unexpected results of the activity assay show that the lockdown mutant is insensitive to DTT. These results have caused us to consider several conjectural, yet fundamental, theories as the hypothesis of the project evolves and future work is carried out.

Acknowledgements

I would like to thank my research mentor, Dr. Joanie Hevel, for her insight and guidance throughout the duration of my work in her lab.

I would also like to thank all the other Hevel Lab researchers for their support and comradery. Special thanks to Heather Tarbet for performing the assays involving radioactivity.

Finally I would like to acknowledge and thank URCO for funding this project.

Table of Contents

List of Figures

Introduction

The human body depends on the ability of individual cells to communicate effectively and efficiently with each other in order to function properly. Cellular signaling networks that drive physiological processes are often regulated by enzymatic proteins that transform substrate molecules or even other proteins in ways that change their signaling properties. One vital enzyme family is that of protein arginine methyltransferases.

The duty of protein arginine methyltransferases (PRMTs) is their namesake—methylating protein arginine residues using S-adenosyl methionine (SAM, AdoMet) as a methyl group donor. PRMTs play key regulatory roles in human physiological pathways such as DNA repair and transcription, RNA processing, signal transduction, and protein transport from the nucleus to the cytoplasm[1]. These enzymes have become the subject of great research interest due to the recent elucidation of their involvement in disease conditions. Specifically, asymmetrical dimethylarginine (ADMA), a product of PRMT activity, is an endogenous inhibitor of nitric oxide synthase, an enzyme responsible for the production of nitric oxide which is involved in vasodilation and atherosclerosis prevention[2]. Due to this inhibition, ADMA has been labeled as a novel biomarker in cardiovascular disease[3].

Research has helped uncover the important physiological roles PRMTs play. However, there is inadequate knowledge of the fundamental biochemistry of these enzymes. Particularly, substrate recognition in PRMTs is poorly understood and of great interest in the Hevel lab. We hypothesize that the N-terminus of PRMT1 (one of 11 human PRMT isoforms) is highly mobile and involved in recognizing substrates, aiding in catalysis by virtue of a change in its conformation. The N-terminus has not been visualized in the crystal structure of rat PRMT1 (rPRMT1, the enzyme this project focuses on), lending support to the notion of its mobile nature. In my research I attempted to assess that motion and its physiological relevance by mutating serine 31 (N-terminal) and lysine 127 (core residue, near the active site) to cysteine residues (see **Figure 1**). These cysteine residues were to be manipulated by forming a disulfide bond between them, locking down the N-terminus and preventing it from moving freely. In this "locked down" conformation, activity of the enzyme was expected to be abolished. Crystallization attempts of the lockdown mutant and hopeful elucidation of a crystal structure by x-ray diffraction with the N-terminus of rPRMT1 visible remain as future work in the lab.

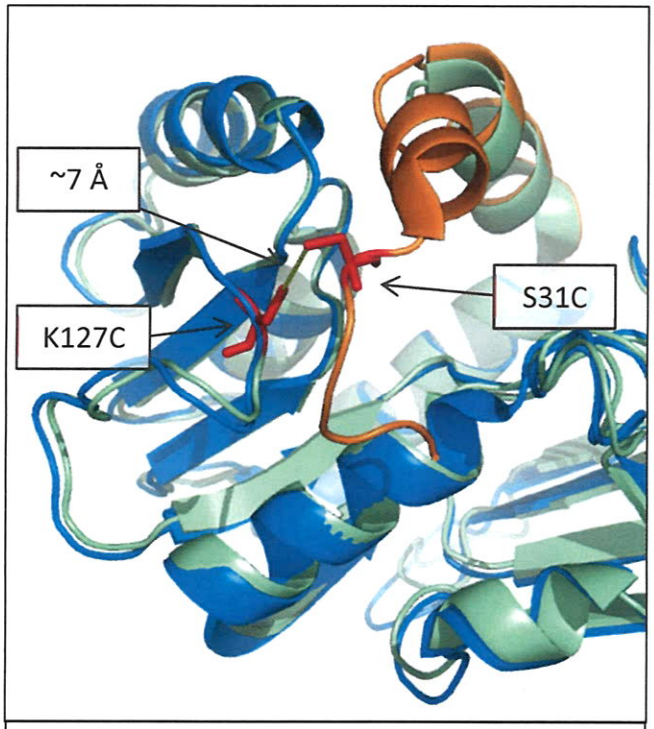

Figure 1. Approximation of PRMT1 N-terminal tail. Structures of rPRMT1 (PDB 1OR8, green) and rPRMT3 (PDB 1F3L, blue) were overlaid *in silico* in order to approximate an N-terminal residue within PRMT1 that would be a viable candidate for cysteine mutagenesis. The N-terminus of PRMT3 is shown in orange for visual emphasis.

Methods & Materials

A construct of full-length rPRMT1with an N-terminal histidine tag had been previously created in the lab and inserted into a pET-28b vector[4]. This was used as the template for site-directed mutagenesis.

Mutagenesis primer design.

By using the known sequence of the rPRMT1 gene, DNA primers that contained specific base-pair alterations were designed to facilitate site-directed mutagenesis. Codon mutations were designed for amino acids K127, E129, and S31. Each codon was changed to a cysteine codon (see **Table 1**).

Table 1. Codon mutations included in mutagenesis primers.

Amino Acid	Codon	Mutation
K127	AAG	TGT
S31	TCC	TGC

PCR: Site-directed mutagenesis.

For the K127C mutation, 1.89μL (60ng) vector was first digested with 1μL NdeI in 2μL 10X FastDigest Buffer and 15.11μL water (total reaction volume 20μL) for 45 minutes at 37°C. 10μL of the digest reaction was then ligated in 4μL 5X rapid ligation buffer, 1μL T4 DNA ligase and 5μL water (total 20μL). The ligation reaction was incubated at room temperature for 10 minutes. This protocol was done in order to reduce supercoiling and increase polymerase efficiency. PCR clean-up of the ligated template was performed, following Qiagen protocol. Next, the PCR reaction was prepared by mixing 0.5μL (125ng) forward primer, 0.33μL (125ng) reverse primer, 1μL (15ng) template, 5μL 10X Buffer, 2μL dNTP mix, and 1μL Pfu turbo DNA polymerase in 40.17μL water (total volume 50μL). The PCR reaction was run in a BioRad thermocycler according to the scheme displayed in **Figure 2**. After PCR, 1μL DpnI was added to the reaction mixture and incubated at 37°C for 1 hour.

After the DpnI digest, 5μL of the reaction was incubated with 50μL XL1-Blue E.coli cells on ice for 20 minutes. The mixture was heat shocked for 45 seconds at 42°C, followed by 2 minutes of incubation on ice. 450μL SOC broth were added to the mixture and the entire volume was shaken for 1 hour at 37°C. The shaken growth mixture was then centrifuged for 3 minutes at 1800 rpm. 375μL supernatant was removed. The cell pellet was carefully resuspended in the remaining broth and plated on agar containing kanamycin (KAN) and left to grow overnight at 37°C. The resulting colony was picked and grown overnight in 5mL LB media with 15μL KAN. The growth was shaken at 37°C. Qiagen plasmid prep protocol was then followed to extract the DNA from the cells and the resulting extract was sent the Center

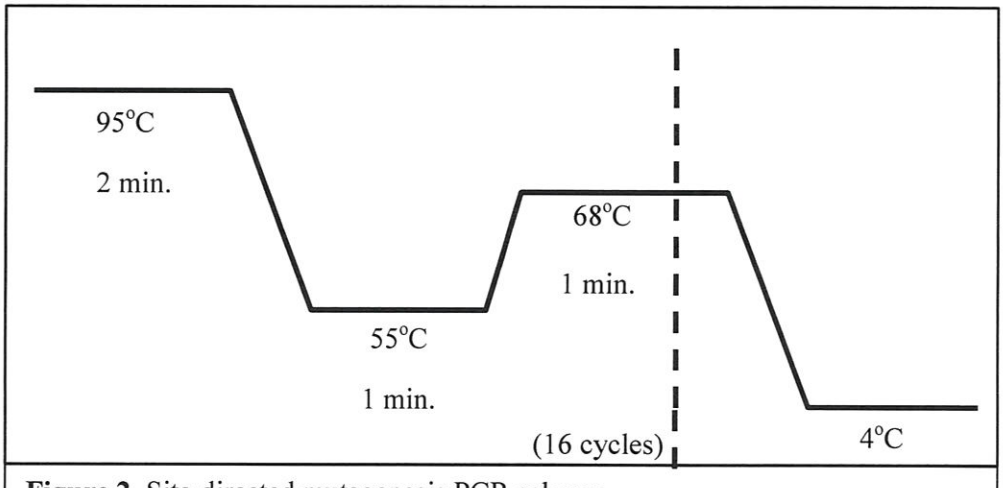

Figure 2. Site-directed mutagenesis PCR scheme.

for Integrated Biosystems (CIB) for sequencing.

For the S31C mutation, the reaction mixture was prepared by mixing 5μL 10X buffer, 15ng K127C mutant template, 125ng forward primer, 125ng reverse primer, 2μL dNTP mix, and 1μL Pfu turbo DNA polymerase in 40.57μL water (total volume 50μL). PCR thermocycler program, DpnI digest, transformation and plasmid preps were the same for S31C as K127C, with the exception of using DH5-alpha cells in place of XL1-Blue cells. DNA extracts were sent to CIB for sequencing.

Protein expression test.

50μL BL21 E.coli expression line cells were transformed with 2μL (7.5ng) S31C-K127C mutant vector, following same transformation protocols as before (with exception of cell line difference). 100μL of broth mixture was plated for colony isolation. Resulting colony was picked and grown overnight in the shaker (5ml LB media, 15μL KAN). Two (2) 50mL flasks of LB media were then each inoculated with 500μL of growth mixture and an additional 150μL KAN. These were shaken at 37°C until optical density of 0.6 was reached, and then inoculated with 29.8μL IPTG (0.5mM). One flask remained at 37°C, while the other was placed at room temperature. Both growths were shaken and 1mL samples were taken at timepoints of 5, 20, and 24 hours. The samples were centrifuged for 3 minutes at 2200 rpm, supernatant discarded and resultant pellets stored at -20°C until further analysis was to be performed.

Sample pellets were resuspended in 250μL lysis buffer (500mM NaCl, 20mM imidazole, 50mM NaPO4, pH 7.5, filtered) and lysed by sonication. Lysed cell mixtures were centrifuged at 4oC for 25 minutes at 14,000 rpm. Supernatants were retrieved and samples were prepared for SDS-PAGE (5μL 4X dye, 15μL supernatant. 50μL 4X dye, cell pellet). The SDS-PAGE samples were boiled for 5 minutes in a 100°C sand bath. SDS-PAGE was performed, the gel stained with coommassie, and the resulting gel was imaged for records.

Nickel resin purification test.

A BL21 colony transformed with the mutant plasmid was used to start a 5mL hot culture growth. 1mL of this growth was added to 500mL LB media along with 1.5mL KAN. The mixture was incubated at 37°C until an optical density of 0.6 was reached. The growth was induced with 298μL IPTG (0.5mM) and incubated in the shaker at room temperature for 24 hours. Cells were harvested by centrifugation and stored at -80°C until lysis.

0.5g of cells were resuspended in 1mL lysis buffer (50mM NaPO4, 20mM imidazole, 500mM NaCl, pH 7.5) and lysed by sonication. Lysates were centrifuged for 25 minutes at 14,000rpm and 4°C. Supernatant was separated from the cell pellet and samples were taken for SDS-PAGE. 50μL Ni2+ resin was equilibrated by washing 3 times with 1mL lysis buffer (centrifuged for 4 minutes at 700*xg*). Once equilibrated, the resin was suspended in the remaining supernatant and mixed at 4 oC for 72 hours. Five 300μL washes were performed with washing buffer (50 mM NaPO4, 100 mM NaCl, pH 7.5) with concentrations ranging from 20 mM imidazole to 100 mM imidazole. The batch was eluted with elution buffer (50 mM NaPO4, 100 mM NaCl, pH 7.5) containing a range of imidazole from 150mM to 500mM (6 times, 100μL elutions). Cell pellet, supernatant, flowthrough, washes and elutions were all analyzed by SDS-PAGE.

Mid-scale protein expression and purification.

Transformation.

50µL BL21 *E. coli* expression line cells and 2µL (7.5ng) rPRMT1 S31/K127C mutant vector were mixed and incubated on ice for 30 minutes. The mixture was then heat shocked for 45 seconds at 42°C, followed by immediate incubation on ice for 2 minutes. 450µL SOC were added and the resulting mixture was shaken for 1 hour at 37°C. After shaking, 100µL of the broth mixture was plated on kanamycin (KAN) agar and placed in an incubator at 37°C to grow overnight. After overnight colony growth, agar plate was stored at 4oC for future inoculation use.

Expression.

For starter growth, 50µL 1000X KAN were added to 50mL LB media. This mixture was inoculated with one of the resulting BL21 colonies and shaken for 6 hours at 37°C.

500µL 1000X KAN were then added to 3 x 500mL LB media. The flasks were each inoculated with 5mL starter growth and shaken at 37°C until they reached 0.6 optical density (OD). Flasks were then each induced with 298µL IPTG (0.5mM), and remained in the shaker for 24 hours at room temperature. 4.9g cells were harvested by centrifugation (8000rpm, 15 minutes, 4°C) and stored at -80°C until further work was to be performed.

Cell growth and protein purification.

4.9g BL21 *E.coli* cells containing rPRMT1 S31/K127C lockdown mutant were resuspended in 15mL lysis buffer (50mM NaPO4, 500mM NaCl, 20mM imidazole, pH 7.5) and lysed by sonication. Resulting lysate was centrifuged (20,000rpm, 20 minutes, 4°C) and supernatant was separated from cell debris pellet. 500µL Ni Sepharose affinity resin were equilibrated by washing three times with 1.5mL lysis buffer (all resin centrifugation was performed at 700*xg*, 5 minutes, 4°C). After equilibration, Ni resin was resuspended in lysate supernatant and mixed for 2 hours at 4°C.

The loaded resin was then washed with 2 x 10mL lysis buffer, followed by 5 x 10mL washing buffer (50mM NaPO4, 100mM NaCl, pH 7.5) containing imidazole in concentrations of 20mM, 40mM, 50mM, 70mM and 100mM, respectively. The batch was then eluted with 6 x 2mL elution buffer (50mM NaPO4, 100mM NaCl, pH 7.5) containing imidazole in concentrations of 150mM, 200mM, 250mM, 300mM, 400mM and 500mM, respectievly. Cell pellet, supernatant, flowthrough, washes and elutions were all analyzed by SDS-PAGE to ensure purity levels.

Elutions were pooled and dialyzed in dialysis buffer (50mM NaPO4, 100mM NaCl, 5% glycerol, pH 7.5) to remove imidazole. Dialyzed elution pool was then concentrated to 1.61mg/mL, beaded in liquid nitrogen and stored at -80°C.

Activity assay.

Three (3) 65µL reactions were prepared, as follows. The first reaction consisted of 5µL rPRMT1 S31/127C (due to the impure nature of the enzyme, 5µL were used to approximate 100nM concentration), 2µM hnRNPK (substrate), 50mM NaPO4, 0.522µM radiolabeled SAM (*S*-adenosyl-l-[methyl-3H]methionine, [3H]SAM), and dH2O up to volume. The second reaction consisted of the same components as the first reaction, with the addition of 1µM dithiothreitol (DTT). The third reaction also mirrored the first reaction, but replacing the mutant protein with 70nM WT rPRMT1. The three reactions were incubated at 37°C and 30µL samples were taken at 15 and 30 minutes. Reactions were stopped by boiling the time point samples with 8µL 4X XT Bis-Tris sample buffer (Bio-Rad) for 5 minutes. Boiled samples were run on a 10% CriterionTMXT Bis-Tris precast gel and transferred to a Polyvinylidene

Flouride (PVDF) membrane. The membrane was treated with En3Hance according to manufacturers' instructions. PVDF membrane was then incubated with film at -80°C for 2 weeks. Film was developed using Kodak® developer and fixer according to manufacturers' instructions, and photographed for analysis.

Results & Discussion

CIB sequencing.

Sequencing results received from CIB were aligned with the sequence of the wild type PRMT1 gene to verify successful mutagenesis. Several attempts were made until the K127C mutation was achieved, followed by the S31C mutation.

Expression Test.

The expression test was performed to find out the optimal growth conditions for expressing the mutant protein. In order to do so, SDS-PAGE was performed on lysate samples of cells grown in different temperatures and for different amounts of time. The SDS-PAGE gel elucidated which conditions were most favorable for expression, as detailed in **Figure 3**. As seen in the gel, there is a protein band at the approximate weight of rPRMT1 (~40kDa) in the cell lysates, which provides supporting evidence that the mutant protein was indeed expressed. Also it suggests that the protein is stable, and doesn't degrade. The most viable condition was determined to be 24 hours growth at room temperature after IPTG induction. These parameters were used to grow cells for a mini nickel resin purification test, and will be used for large scale growth and expression of the mutant protein.

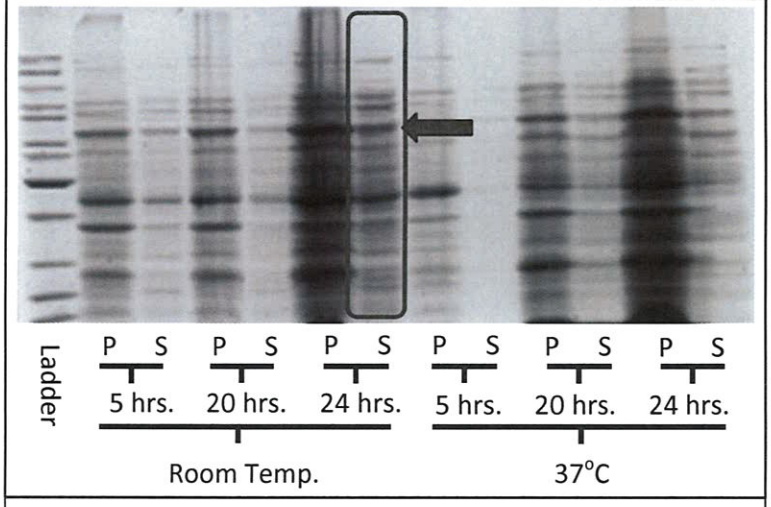

Figure 3. SDS-PAGE analysis of lockdown mutant expression tests. Expression tests at varying times and temperatures were performed to verify expression viability of and elucidate optimal expression conditions for the mutant protein in *E. coli*. The red box indicates the supernatant sample taken from the 24 hour room temperature growth. This condition was chosen due to the higher amount of soluble lockdown mutant, indicated by the red arrow.

Nickel resin purification test.

Once expression viability was determined in the expression test, a mini purification test was run to determine whether or not the protein could be purified for further analysis. Nickel resin was used because the histidine tag interacts with the nickel atoms that are ligated to the resin, and other lysate components will flow through. Samples of the washes and elutions were analyzed by SDS-PAGE (**Figure 4**). As seen on the gel, the mutant protein was bound to the nickel and then eluted with increasing concentrations of imidazole. This means that nickel resin is a viable option for large scale purification of the mutant protein, and the concentration parameters used in this "mini-prep" will be used as standards in

future large scale work. However, the protein is not completely pure, and additional purification steps should be taken to increase purity.

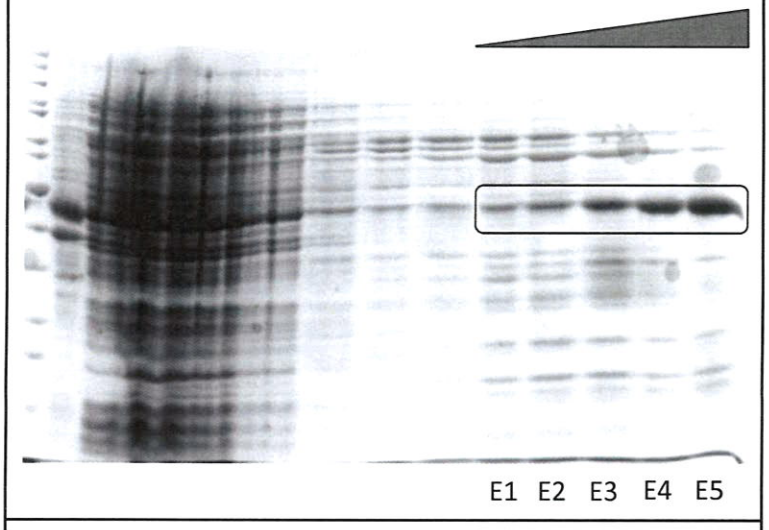

Figure 4. SDS-PAGE analysis of small-scale nickel purification. Red box emphasizes the elution of the lockdown mutant as concentration of imidazole increases in E1-E5. The presence of contaminants in the elutions warrants the performance of additional purification steps.

Mid-scale expression and protein purification.

After having establishing basic parameters for the expression and purification of the lockdown mutant, the process was up-scaled in order to obtain amounts of protein viable for activity analysis and crystallization experimentation. SDS-PAGE was performed on the resulting cell growth and protein purification steps outlined in the methods section above. **Figure 5** details the SDS-PAGE gel obtained from running samples of cell pellet, supernatant, flowthrough, washes and elutions. This form of analysis lent further support to the viability of the expression and purification steps taken to obtain the mutant lockdown protein. As seen in the gel, with increasing concentrations of imidazole, the rPRMT1 mutant elutes in increasing amounts. Due to purposefully overloading the Ni resin this SDS-PAGE gel differs from previous purification PAGE results in that the protein appears to be clean after a single pass over nickel resin. When testing for purification viability last semester other contaminants were visible in the elutions after staining. More resin could have been used, capturing not only more target protein, but contaminants as well. Since this was a mid-scale growth and purification,

Figure 5. SDS-PAGE analysis of mid-scale nickel purification. Red box emphasizes the elution of the lockdown mutant as concentration of imidazole increases in E1-E4. The seeming lack of contaminants is due to overloading the nickel resin, preventing contaminants from binding.

these considerations will be taken into account in the future large-scale protocols used to obtain this protein, and additional purification steps will be taken as needed to ensure adequate purity levels.

In addition to purifying the protein, steps were taken to increase concentration in an attempt to reach crystallization standards. However, due to the overloading of the resin, not all the protein was salvaged from the growth. As such, the resulting concentration (1.61 mg/mL) was not high enough for crystallization attempts (~10mg/mL).

Activity assay.

The other aim of the project was to observe changes in enzymatic activity in the lockdown mutant by manipulating the mutated cysteine residues. This aim was pursued by performing an assay in which the lockdown mutant was provided with substrate (hnRNPK) and a radiolabeled methyl donor ([3H]SAM). If the enzyme were active and able to methylate its substrate, the tritiated methyl group of [3H]SAM would be incorporated in the methylated product, and a band of corresponding weight would develop on an autoradiography film. Conversely, if the enzyme were unable to methylate its substrate, there would be no methyl group incorporation and no band would develop on the film. Reactions were allowed to run in the presence and absence of DTT, hoping to see a lack of methylation in the absence of DTT (mutant disulfide bond in place, N-terminus in the "lockdown" conformation), and methylation in the presence of DTT (mutant disulfide bond reduced, N-terminus in "free" conformation). A methylation reaction using wild-type rPRMT1 was also run as a control. The resulting film obtained from this portion of the experiments is detailed in **Figure 6**. Bands denoting radiolabel incorporation via methylation developed in all reaction mixtures. The results were not what we expected to see, yet important inferences are to be made from the data, and there are several conjectural theories that might explain what is occurring. Before exploring these possibilities, it is important to note that since the concentration of the mutant used in the assay was approximated, it cannot be concluded that this mutant is more active than WT.

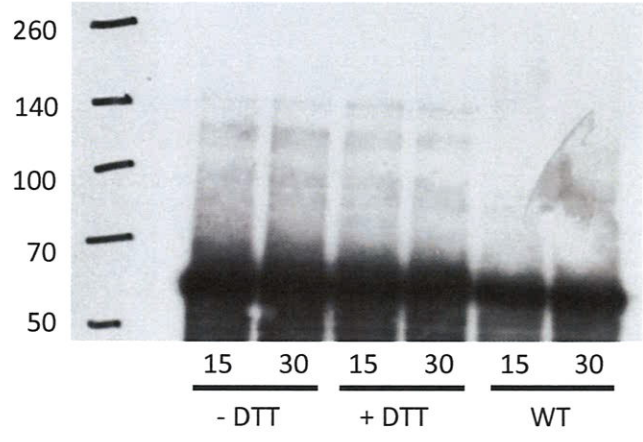

Figure 6. Autoradiography film showing methylation activity of mutant and WT rPRMT1. The series of bands spanning the film correspond to radiolabel incorporation into the substrate hnRNPK, and thus enzyme activity. The lockdown mutant was equally active in both the absence (-DTT) and presence (+DTT) of the reductant dithiothreitol.

It is apparent that the reductant DTT does not have any effect on the activity of the mutant. Unpublished results from studies performed in the Hevel lab show that WT his-rPRMT1 is more active in the presence of DTT, so something has changed within the mutant that has altered its sensitivity to DTT. Formation of an unintended disulfide may disrupt WT disulfide formation elsewhere in the enzyme. We were able to explore this possibility by highlighting all of the natural occurring cysteine residues within the rPRMT1 structure. We discovered that there is another cysteine residue (C101) near the active site

pocket which lies adjacent to the K127C mutation (**Figure 7**). These two residues lie in such proximity to each other that they may be able to form an unintended disulfide bond, preventing the hypothesized S31/K127C disulfide.

Additionally, there are two other naturally occurring cysteine residues within the N-terminus of PRMT1, C9 and C15 (these residues are not visible in the crystal structure, nor are there enough residues visible in the PRMT3 Nt structure to approximate their relative location). These cysteines may participate in normal WT activity. If the formation of the hypothesized—or unintended—disulfide disrupts those interactions, then differences in behavior from WT are to be seen.

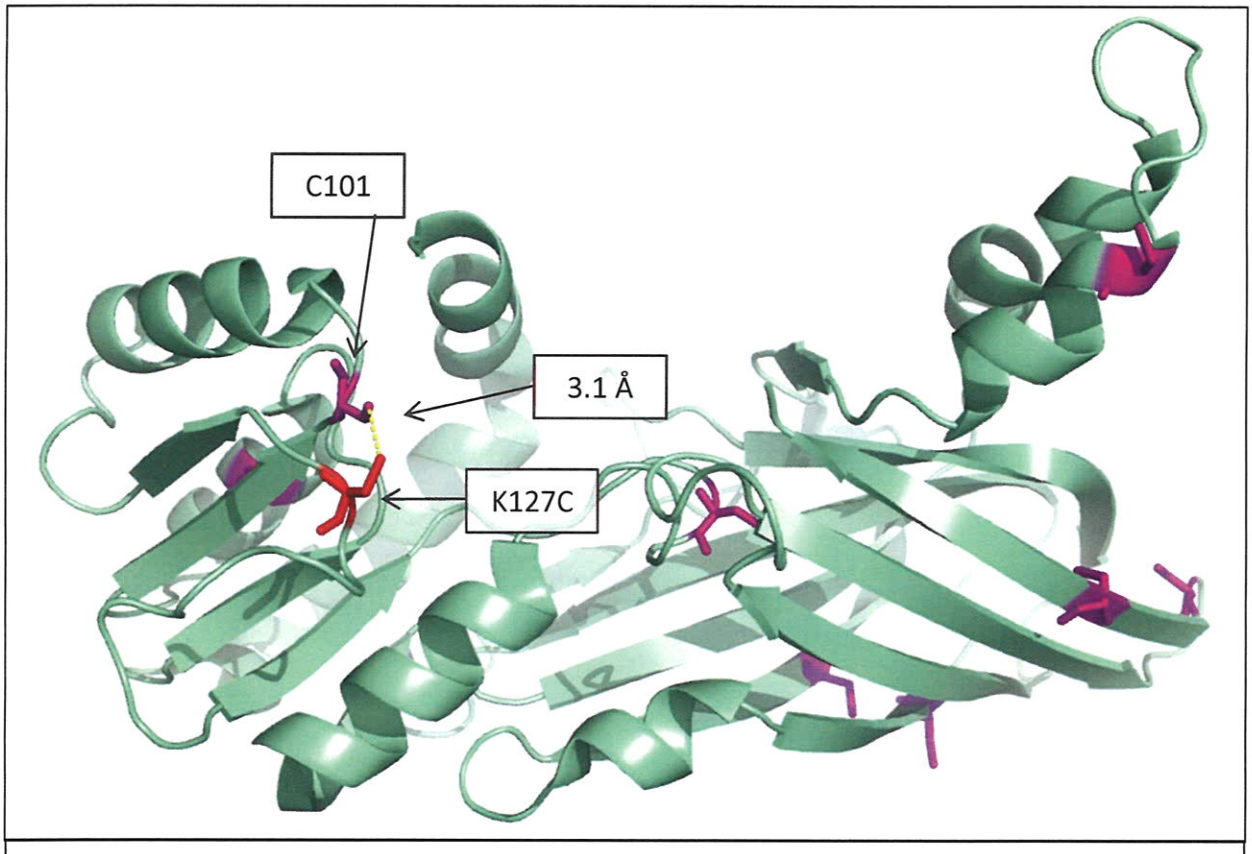

Figure 7. Cysteine residues in PRMT1. Naturally occurring cysteine residues (magenta) and the K127C mutant cysteine (red) are highlighted in the rPRMT1 crystal structure (PDB 1OR8). As emphasized, C101 lies in close proximity to K127C (3.1 Å), which may facilitate unintentional disulfide formation between these two residues.

Conclusions & Future Work

It is clear that we still lack a great deal of understanding of how the N-terminus behaves. However, important discoveries were made with respect to the project, and will aid greatly in investigating our evolving hypotheses regarding the N-terminus of PRMT1. Future work with this lockdown mutant includes performing additional activity assays in the presence of oxidant to aid in disulfide bond formation between the mutant cysteine residues. Also, obtaining purified rPRMT1 S31/K127C mutant at high enough concentrations to attempt crystallization is high priority, as locking down the N-terminus may lead to its visibility within a crystal structure. All of this work will aid in the pursuit of uncovering the role the N-terminal tail of methyltransferases and how they can be manipulated in beneficial ways.

References

1. Weber, S., et al. (2009). PRMT1-mediated arginine methylation of PIAS1 regulates STAT1 signaling, *Genes Dev.* **23**, 118-132.

2. Atenzi, F., et al. (2010). Usefulness of cardiovascular biomarkers and cardiac imaging in systemic rheumatic diseases. *Aut. Rev.* **9**: 12, 845-848.

3. De Gennaro Colonna, V., et al. (2009). Asymmetric dimethylarginine (ADMA): an endogenous inhibitor of nitric oxide synthase and a novel cardiovascular risk molecule. *Med. Sci. Monit.* **15**: 4, 91-101.

4. Zhang, X., et al. (2003) Structure of the Predominant Protein Arginine Methyltransferase PRMT1 and Analysis of Its Binding to Substrate Peptides. *Structure*. **11**: 5, 509-520.

5. Cheung, N., et al. (2007) Protein arginine-methyltransferase-dependent oncogenesis. *Nature*. **9**: 10, 1208-1215

6. Di Lorenzo, A., et al. (2010) Histone arginine methylation. *FEBS Lett*.

7. Nicholson, T., et al. (2009) The physiological and pathophysiological role of PRMT1-mediated protein arginine methylation. *Pharm. Res.*, **60**: 6, 466-474

8. Bedford, M., et al. (2009) Protein arginine methylation in mammals: what, what and why. *Mol. Cell.*, **33**: 1, 1-13.

9. Wolf, S. (2009) The protein arginine methyltransferase family: an update about function, new perspectives and the physiological role in humans. *Cell. Mol. Life Sci.*, **66**: 13, 2109-2121.

Author's Biography

Taylor Rasmussen grew up in Parowan, Utah and graduated from Parowan High School in 2005. He came to Utah State University as a Presidential Scholar studying Engineering with a pre-pharmacy mindset. He was awarded the Balanced Man Scholarship by the Sigma Phi Epsilon fraternity. After his first year at USU, he took a brief leave of absence to serve a mission for the LDS church in the Dominican Republic. Upon his return to USU in 2008, he changed his major to Biochemistry with a Spanish minor and continued his studies until graduating in the spring of 2012. As an undergraduate he pursued Departmental Honors and performed undergraduate research in the lab of Dr. Joanie Hevel in the Department of Chemistry and Biochemistry at USU. He was awarded an URCO Grant for his research efforts. He also received licensure and secured employment as a pharmacy technician in the State of Utah during his time as an undergraduate.

Taylor intends to pursue a Doctor of Pharmacy degree following graduation, and upon finishing will serve committedly and faithfully in the pharmacy field.